

Chapter 22

The Quadrifilar Helix Antenna

Sec 22.1 Introduction

The quadrifilar helix antenna, shown in Fig 22-1, is seeing use on commercial and military, as well as amateur spacecraft. For amateur applications it first saw use on AMSAT-OSCAR 7 in November 1974. I prepared the basic information in this chapter while I was employed as an antenna engineer at RCA's Astro-Electronics Division in Princeton, New Jersey. Information also appears in Chapter 20 of *The ARRL Antenna Book*, 15th edition (Ref 71). While working at RCA, I assisted in the development of the quadrifilar helix.¹ We consider this antenna to be an outstanding contribution to practical spacecraft antenna engineering from the viewpoint of flexibility in design. The quadrifilar helix provides a large range of radiation characteristics from a radiator of extremely small size and weight, from which we can select a pretested design to match the radiation requirements of any particular spacecraft.

The quadrifilars shown in Fig 22-1 are flight-model units for operation at 1800 and 2200 MHz. I also assisted in the design of quadrifilars for 121.5, 243, and 1600 MHz, which are flying on TIROS-N (NOAA 9 through 14) weather spacecraft in the worldwide Search and Rescue (SAR) Emergency Locator Transmitter (ELT) service. The service is primarily for downed or stricken aircraft, over either

land or sea.

One reason for presenting details of the quadrifilar in this book is that it is an inherently excellent antenna for ground station use in the amateur satellite service. Once you study the following engineering aspects of the quadrifilar, you'll discover its advantages over other circularly polarized antennas, such as crossed Yagis. It is useful at 144 MHz, and up, and all the critical dimensions are included in this chapter. The dimensions are listed in wavelengths, so all you have to do is convert them to the desired frequency. The details of feeding, phasing, and infinite balun construction are given in the drawings and photos, long with sufficient explanation for you to construct your own quadrifilar.

Radiation from the quadrifilar helix antenna is circularly polarized and of the same screw sense everywhere throughout the radiation sphere. The antenna embodies a unique configuration and method of feeding loop elements to produce radiation having a controllable pattern shape. Refer again to Fig 22-1. The quadrifilar antenna comprises two bifilar helical loops oriented in a mutually orthogonal relation on a common axis. The terminals of each loop are fed 180° out of phase, and the currents in the two loops are in phase quadrature (90° out of phase).

By selecting the appropriate configuration of the loops, a wide range of radiation pattern shapes is available, with ex-



Fig 22-1 — Two flight-model quadrifilar helix antennas. The larger is for use around 1800 MHz, and the smaller around 2200 MHz. Radiation from each antenna is circularly polarized and of the same screw sense everywhere throughout its radiation sphere.

cellent axial ratio appearing over a large volume of the pattern. The basic form of the quadrifilar antenna was developed by Dr C. C. Kilgus of the Applied Physics Laboratory, Johns Hopkins University, who has published several papers that establish the theoretical basis for its operation. (*See Refs 88 through 96*). The Brown and Woodward citation (*Ref 90*) is especially helpful in understanding the radiation characteristics of the quadrifilar. That paper describes radiation from the combination of a dipole and a circular loop sharing a common axis, and fed in phase, which produces radiation characteristics similar to the quadrifilar. This version of the quadrifilar helix uses a

novel feed system that includes the infinite balun. The feed system also includes a means for attaining the required 90° differential current phase relationship without requiring additional components to achieve separate differential-phase excitations.

The quadrifilar antenna is applicable for general use in the frequency range above 30 MHz. It is especially attractive for certain spacecraft applications because it can provide omnidirectional radiation in a single hemisphere (a cardioid volume of revolution) without requiring a ground plane. This no-ground-plane feature affords a dramatic saving in weight and space. In addition, the inherent cardioid

radiation characteristic that eliminates the need for the ground plane also affords freedom in the choice of a mounting position on a spacecraft. The profile of the volume beneath the antenna has relatively little effect on the radiation pattern, provided that the quadrifilar is mounted at least $\lambda/4$ above conducting surfaces which would form a reflective plane.

Quadrifilars designed to operate in the frequency range of 1800 and 2200 MHz can be extremely light, weighing only about 0.7 ounce. Developed by RCA Astro-Electronics, several of these antennas are flying on U.S. Air Force satellites of the Defense Meteorological Support program, also built by RCA. A slightly smaller version of similar design (donated by RCA Astro-Electronics) is the 2304.1-MHz beacon antenna, which flew on AMSAT-OSCAR 7.

Quadrifilars having a somewhat different configuration from that shown in Fig 22-1 have also been developed by RCA for use on RCA-built NOAA TIROS-N weather satellites. The design differs because the radiation pattern requirements are different. The design of the quadrifilars for transmitting the principal video signals from the TIROS-N spacecraft is noteworthy because the radiation pattern has been shaped to maintain a nearly constant signal level versus slant-range distance between the spacecraft and the ground station during the in-view portion of the spacecraft orbit. (RCA-built TIROS-N, or NOAA spacecraft launched around 1979 are still in service today, in April 1999.)

Sec 22.2 Physical Characteristics

There is a tendency to confuse the quadrifilar with the conventional helical antenna, probably because portions of the quadrifilar are helically shaped. As a re-

sult, the radiation characteristics of the quadrifilar antenna are sometimes misunderstood. Although the term quadrifilar is not incorrect, the term itself often fails to conjure up a true picture of the physical characteristics. Therefore, since several characteristics of the quadrifilar antenna differ radically from those of the conventional helical antenna (for example, opposite screw sense of circular polarization), the following paragraphs examine some aspects of both the physical and the radiation characteristics of the quadrifilar to clarify the confusion.

In describing the physical characteristics of the quadrifilar, I will concentrate on the simple half-turn $\lambda/2$ configuration. As I stated earlier, the quadrifilar helix is a combination of two bifilar helicals arranged in a mutually orthogonal relationship along a common axis, and enveloping a common volume.

What is a bifilar helix? One way of visualizing the half-turn $\lambda/2$ bifilar helix is to develop it from a continuous square loop of wire one wavelength in perimeter, as shown in Fig 22-2. As in the driven element of the conventional cubical quad antenna, each side of this square loop is $\lambda/4$, and the feed terminals are formed by opening the loop at the midpoint of the bottom side. We call this square-loop configuration a zero-turn, $\lambda/2$ bifilar loop. There is a half wavelength of wire radiator extending away from each feed terminal around the loop to the antipodal point on the opposite side of the square (loop half-length l_{en}° equals $\lambda/2$). The drawing shows length l_{en}° with a script letter L. This loop is a balanced input device, requiring a balanced, two-wire feed line with push-pull currents.

To visualize the development of the quadrifilar helix, imagine inserting an imaginary cylinder of diameter $D = \lambda/4$ inside the loop. Then, while holding the

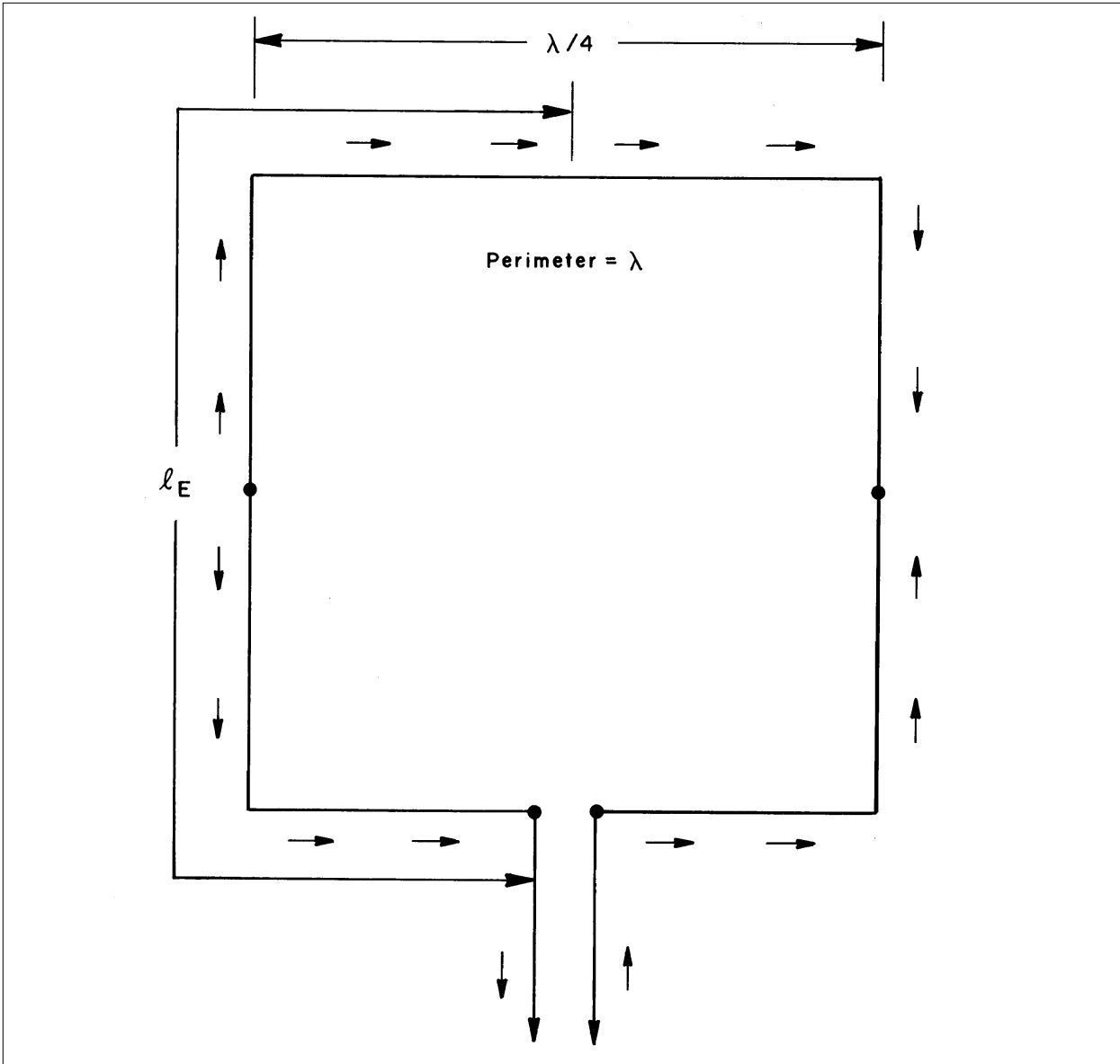


Fig 22-2—Horizontally polarized square loop radiator. The small arrows represent the direction of current flow.

bottom side of the loop fixed, grasp the top side and give it a half turn of rotation with respect to the bottom. As a result, shown in Fig 22-3, each of the two vertical sides of the square loop becomes a half-turn helix as it curves around the surface of the imaginary cylinder. However, because of the curved paths of the once-straight vertical sides, the distance between the top and the bottom has shrunk, and the axial length, len_p° , is less than the $\lambda/4$ diameter.

With these particular proportions of

the 1/2-turn, $\lambda/2$ bifilar, some of the radiation characteristics are not particularly attractive. However, some physical parameters of the loop may be selected to obtain characteristics that make this antenna especially attractive. Such parameters include the electrical length of the conductors, the number of turns, the cylindrical diameter D , and length len_p° . In addition, for a given conductor length, the length-to-diameter ratio, abbreviated len/diam , of the cylinder is also an important variable, controlled by the diameter and

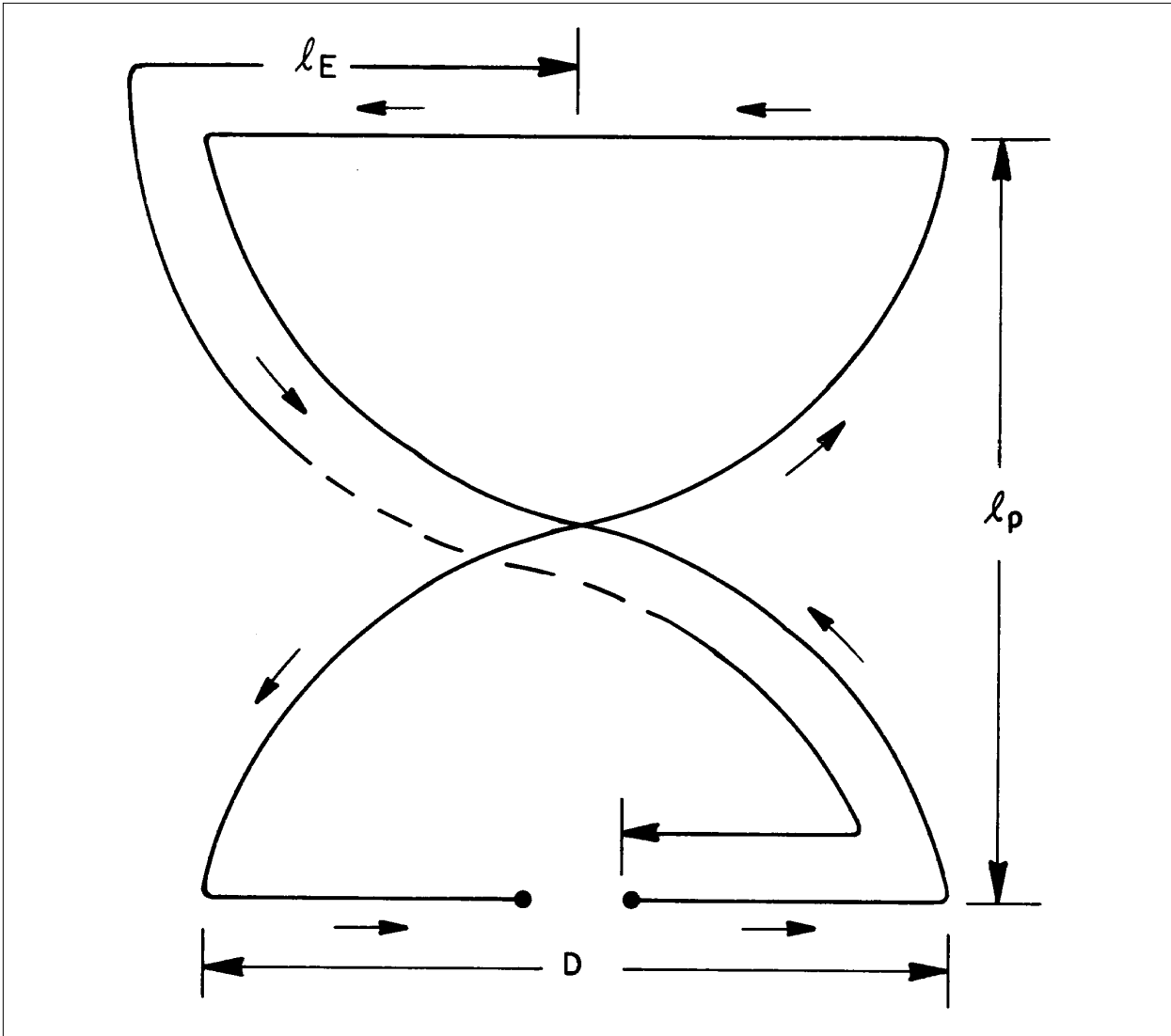


Fig 22-3—Half-turn bifilar helix loop. Distance $l_{E^{\circ}}$ equals the loop half-length.

number of turns. For example, the antennas shown in Fig 22-1 are 1/2-turn, $\lambda/2$ quadrifilars. But by reducing the diameter from 0.25λ to 0.18λ for this model, the axial length is inherently increased to 0.27λ . This results in vastly improved radiation characteristics.

Sec 22.3 Electrical Characteristics

Let's take a short qualitative look at some basic changes in the radiation pattern that result from the 1/2-turn twist of the square loop. First, recall that the square loop having a perimeter $P = I\lambda$ is basically a broadside array of two dipole

elements, with the top element being voltage fed from the bottom element. In this loop the currents in the top and bottom sides flow in the same direction, as shown in Fig 22-2. The horizontally polarized fields produced by the currents in both top and bottom sides are therefore in phase. The two fields add to form the conventional figure-8 broadside radiation pattern. The bidirectional lobes in the pattern are at right angles to the plane of the loop. The null in the pattern appears bidirectionally on a horizontal line that is in the plane of the loop midway between the top and bottom sides.

In the vertical sides of the loop, the

current in the top half of each side flows in the direction opposite to that in the corresponding bottom half. Consequently, the vertically polarized fields produced by both halves of each vertical side are mutually out of phase, and add to zero in all directions. This cancellation of the vertical fields results in zero net vertically polarized radiation.

On the other hand, in the bifilar helix loop having the half-turn twist, the currents in the top and bottom sides flow in opposite directions because of the physical half-turn rotation of the top side. This current relationship is shown in Fig 22-3. Thus, the fields produced by the currents in the top and bottom sides are now out of phase with each other, forming an end-fire array relationship.

In the direction broadside to the plane formed by the top and bottom sides, the fields now cancel completely. As in the ordinary end-fire array, this results in zero radiation in the broadside direction, where maximum radiation appeared with the square loop. The conventional lobes of end-fire radiation contributed by the top and bottom sides now occur toward the top and bottom of the antenna as drawn in Fig 22-3. This radiation is horizontally polarized.

The currents flowing in the helical portions of the loop retain the same current-flow pattern as in Fig 22-2. However, the physical positions of each current segment, or element, in the twisted vertical wires have now been shifted to a new position, and to a new orientation in the helical paths. This results in a corresponding different position and vector direction for each elemental field produced by the helical current elements. As would be expected, the addition of all these elemental fields now results in a composite field consisting of both horizontally and vertically polarized fields.

Sec 22.4 Difference Between Quadrifilar and Conventional Helix

Before considering the radiation characteristics of the bifilar helix further, it may be helpful to mention some critical distinctions between the Kilgus bifilar helix and the conventional helical antenna configurations. In the conventional helical antenna having more than one radiating element, the elements are generally fed in phase. However, Kilgus found that interesting results were obtained with a helical antenna that has two elements spaced radially at 180° when the two elements are fed 180° out of phase. This finding led Kilgus to his further investigation of the bifilar helical antenna having out-of-phase feed, and still further to the quadrifilar configuration. Thus, an alternative way of visualizing the bifilar helix is as a conventional helical antenna with two elements radially spaced at 180° , but with the outer ends radially connected to each other, and with the elements fed *out of phase*.

Dr. Kilgus' analyses provide a more complete theoretical basis for the functioning of both the bifilar and the quadrifilar helix. He shows the current distribution and radiation characteristics of the half-turn, $\lambda/2$ bifilar helix to be similar to those of a loop-dipole combination described by Brown and Woodward (Ref 90). Brown and Woodward analyzed a combination horizontal loop and vertical dipole sharing a common axis. They show that while both a loop and a dipole produce identical toroid shaped radiation patterns, the electric field produced by the dipole current in this arrangement is vertical, and the electric field produced by the loop current is horizontal. When the currents in the loop and dipole are in phase, their fields are in phase quadrature, a

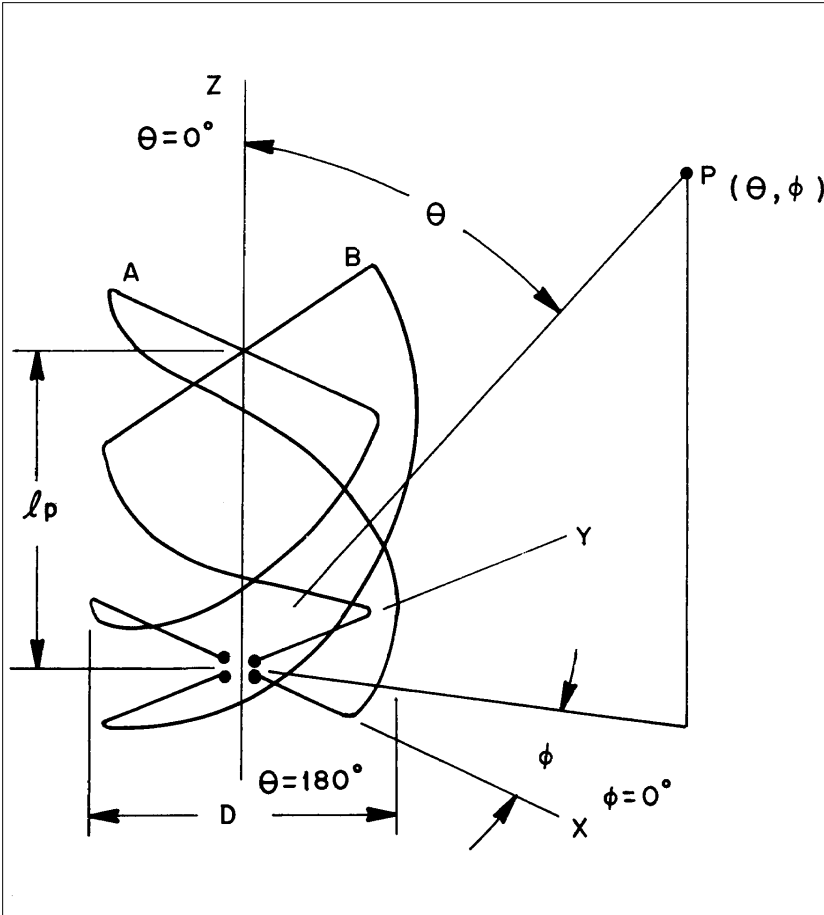


Fig 22-4—Half-turn quadrifilar (two half-turn bifilar loops).

requirement for circularly polarized radiation. When the vertical and horizontal fields are also equal in magnitude, the resulting radiation is circularly polarized, with the same screw sense everywhere throughout the radiation sphere.

Experimental data obtained by Kilgus supports his theoretical analysis, and confirms the similarity of radiation characteristics between the half-turn, $\lambda/2$ bifilar helix and the loop-dipole combination. For the purpose of obtaining additional data pertinent to the development of quadrifilar antennas for use on the TIROS-N spacecraft, I performed extensive measurements of pattern shape, polarization, axial ratio, and terminal impedance on more than a thousand different bifilar and quadrifilar helix configurations. The data obtained from these measurements agree with the Kilgus data, adding further validity to the ear-

lier findings as well as extending them.

Sec 22.5 Development of the Quadrifilar Helix Antenna

In this section we examine the intrinsic cardioid, or omnidirectional hemispheric radiation characteristic of the quadrifilar. In doing so, the toroidal radiation pattern of the bifilar helix becomes of initial primary interest. Recall that in the toroidal radiation pattern of the loop-dipole, maximum radiation occurs broadside to the axis, with the null on the axis. On the other hand, as mentioned earlier, maximum radiation from the bifilar loop occurs bidirectionally along the axis of the loop, while the null appears in the direction perpendicular to the plane formed by the top and bottom sides, or radials of the loop. Except for this 90° rotation of the axes, the radiation characteristics of the two antennas are similar.

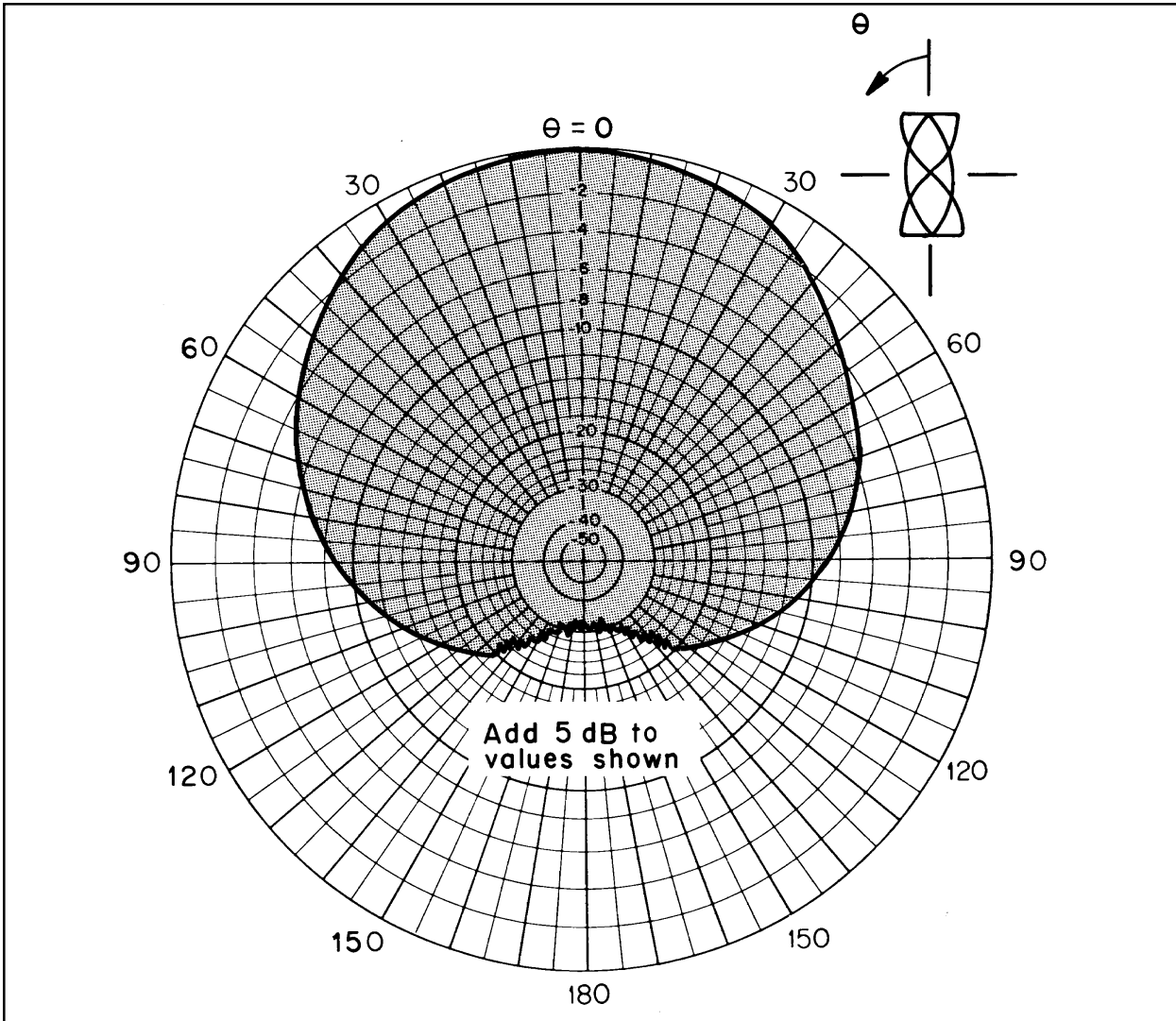


Fig 22-5—Radiation pattern of the half-turn, $\lambda/2$ quadrifilar antenna when illuminated with a circularly polarized source.

We may develop a quadrifilar helix from the bifilar (which I will call bifilar A) by adding a second bifilar, B, on the same axis and enclosing the same space, but rotated 90° relative to bifilar A. This arrangement is shown in Fig 22-4. The fields radiated by bifilar B are identical to those of bifilar A, except that the entire radiation pattern of bifilar B is rotated 90° relative to that of bifilar A. Consequently, the null of bifilar A and the maximum radiation of bifilar B appear at the same point in space, and vice versa. On the other hand, in the axial directions the radiation fields from both bifilars are equal.

This field relationship is the key to the cardioid radiation characteristic of the quadrifilar. When both bifilars are fed in a $0-180^\circ$ and $90-270^\circ$ -phase relationship, respectively, (excited simultaneously with a mutual 90° current-phase relationship), the cardioid radiation pattern appears in the far field. This is because the fields of both bifilars are in phase in one axial direction. In this direction, the two fields add, while in the opposite direction, the fields are out of phase and cancel. As the cancellation is not perfect off axis, the result is a cardioid-shaped pattern of revolution about the axis. In the broadside direction normal to the axis, the respec-

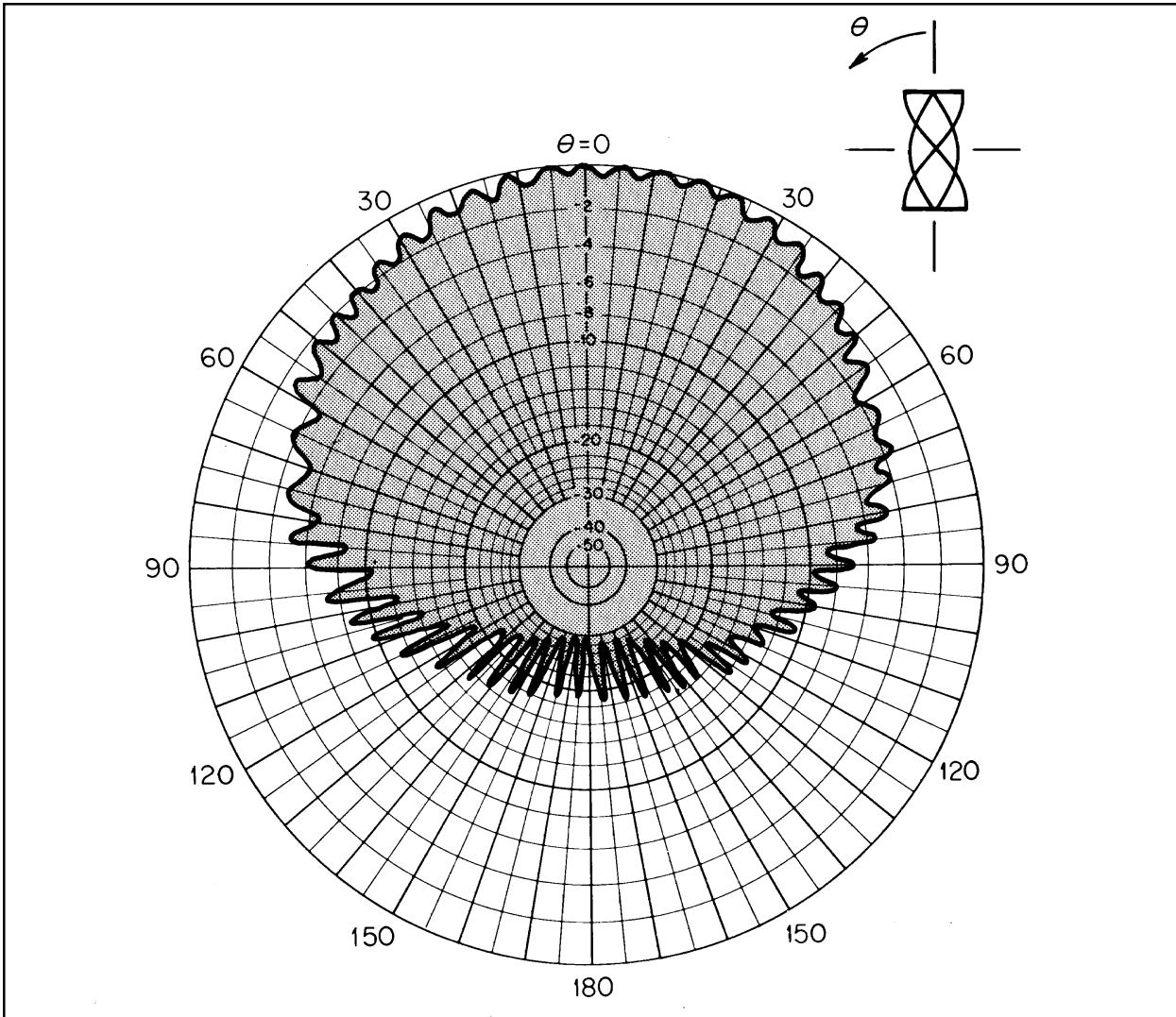


Fig 22-6—Quadrifilar radiation pattern when illuminated with a spinning dipole. This illumination adds axial-ratio data, represented as the difference between adjacent maximum and minimum values of a ripple wave.

tive nulls and maxima of the two individual bifilars compensate each other to produce a uniform omnidirectional radiation pattern around the axis.

See 22.6 The Quadrifilar Shape Factor

As I stated earlier, the radiation pattern shape and the axial ratio of the polarization can be controlled. This is done by tailoring both the length of wire and number of turns in the loop, and the length-to-diameter ratio, len/diam, of the formed cylinder. Kilgus' data shows these relationships graphically for certain

ranges of the parameter values. However, let us now examine how the Air Force 5D, the amateur AMSAT-OSCAR 7 and the TIROS-N quadrifilar designs were tailored to obtain the radiation characteristics required for their particular missions.

When using bifilars having a diameter $D = 0.25 \lambda$, formed by placing a half twist in the square loop of Fig 2, the len/diam ratio is less than one, which yields poor front-to-back and axial ratios. By decreasing the diameter to $D = 0.18 \lambda$ while retaining the half-turn, $\lambda/2$ loop, the axial length increases to $\text{len}_p = 0.27 \lambda$. The resulting ratio, len/diam. = 1.5, yields

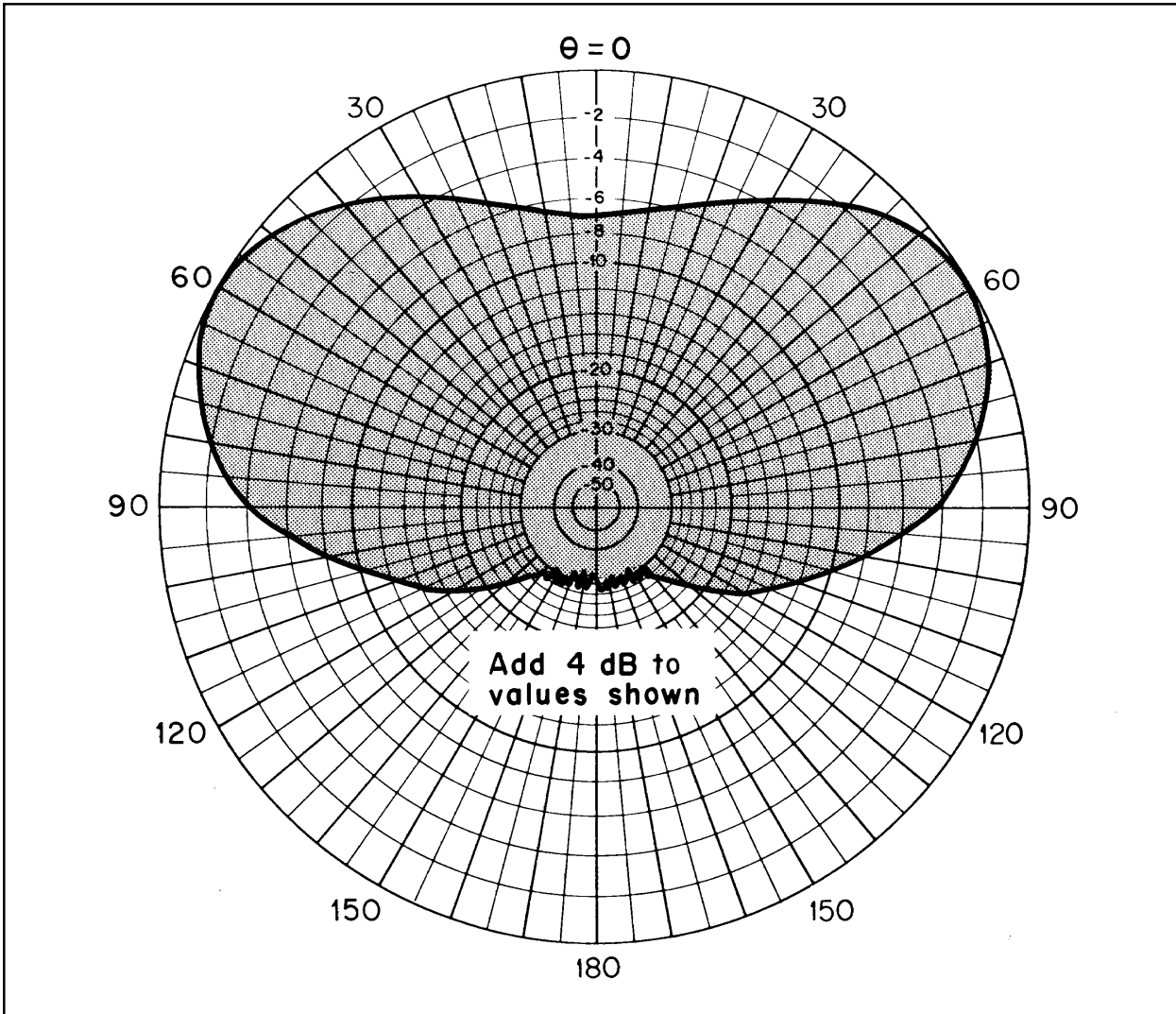


Fig 22-7—Radiation pattern of the 1 1/2 turn, 1.25- λ quadrifilar antenna.

a vast improvement in both front-to-back and axial ratios. These are the design values used in the Air Force 5D and AMSAT-OSCAR 7 quadrifilars. The radiation patterns obtained with this design are shown in Figs 22-5 and 22-6. The patterns are presented in the standard IEEE spherical-coordinate system of notation, and the orientation of the antenna relative to the coordinate axes is shown in Fig 22-4.

The θ radiation pattern shown in Fig 22-5 was measured while using circularly polarized illumination of the quadrifilar. This pattern shows an on-axis gain of 5 dBic (decibels relative to isotropic, circular), and a front-to-back ratio greater than

20 dB. The radiation at any angle θ is uniform for all values of ϕ around the Z axis. Thus, the single θ pattern (at any value of ϕ) represents the shape of the envelope of the volume of revolution about the Z axis, which defines the solid radiation pattern in all directions.

The pattern shown in Fig 22-6 was obtained by using a spinning dipole to illuminate the quadrifilar, to obtain axial-ratio information. The periodic ripple appearing in the pattern results from the rotation of the dipole. The maxima and minima, respectively, correspond to the times when the dipole is parallel to the major and minor axes of the polarization ellipse. The axial ratio may

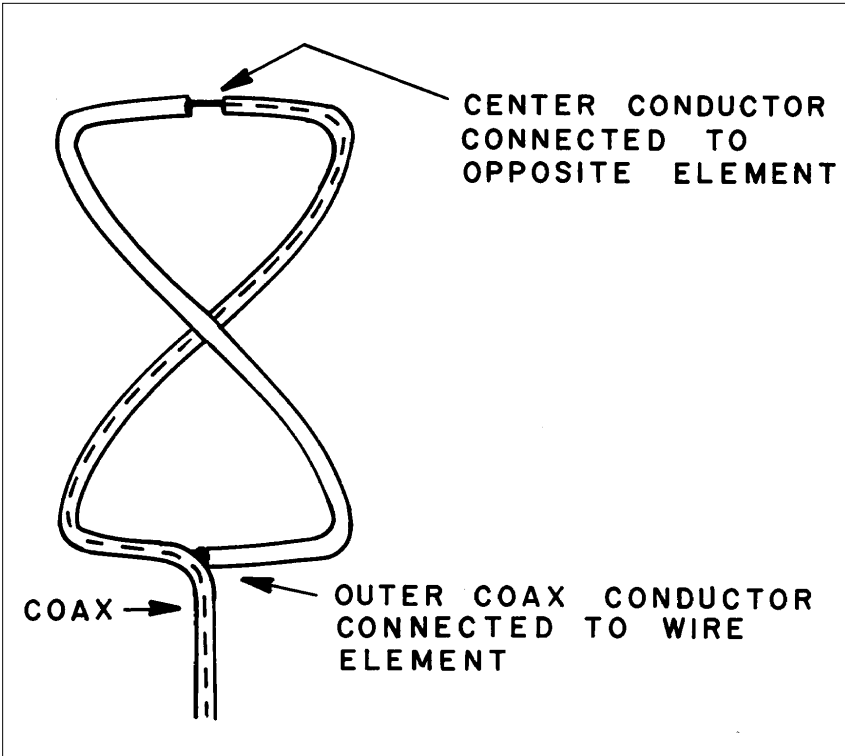


Fig 22-8 — Half-turn bifilar loop with infinite balun ffed.

be determined from the difference between adjacent maximum and minimum values. Thus, the axial ratio of this design is seen to be less than 2 dB over a beamwidth of $\pm 30^\circ$.

As mentioned earlier, the shape-factor parameters for the TIROS-N configuration were determined empirically from the results of my research measurements. I took measurements on more than a thousand combinations of quadrifilar configurations in which each physical parameter was separately varied in small increments while holding the other variables constant. Hundreds of shape-factor combinations were measured, which provided families of patterns from which to select the parameters for the desired pattern shape. The TIROS-N mission required a radiation-pattern shape which provides a nearly constant signal level to the ground station during in-view time. This pattern shape is shown in Fig 22-7. The configuration that yields this radiation pattern was one of the hundreds measured during my research. All

that was required to determine the configuration that would satisfy the radiation-pattern requirements was to search through the hundreds of patterns obtained during the research to find the one that fit the requirements. The bifilar parameters which yield this pattern shape were found to be $1\frac{1}{2}$ turns, 1.25λ loop, $D = 0.1 \lambda \text{ len}_p = 1.0 \lambda$, and $\text{len}/\text{diam} = 10.0$. These quadrifilars, flying on TIROS-N, are used for transmitting weather and other data in the 1600-MHz region, completely separate from the 121.5, 243, and 1600-MHz SAR-ELT quadrifilars flying on the same spacecraft.

See 22.7 Methods of Feeding the Quadrifilar Antenna

Feeding the quadrifilar with a single, unbalanced coaxial line requires special attention. Because the individual bifilar loops are balanced-input devices, some form of balun is required to provide balanced push-pull currents to the terminals of each bifilar. In addition, to obtain the unidirectional radiation characteristic of

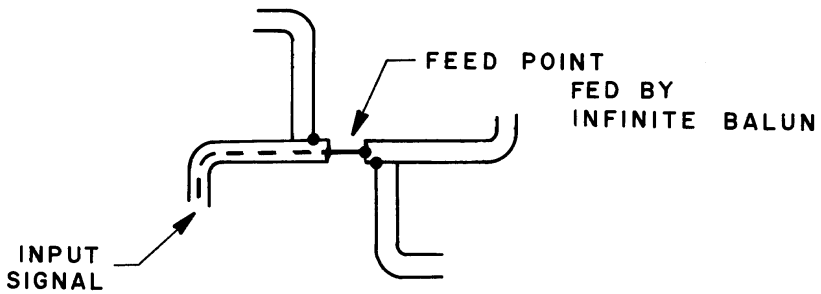


Fig 22-9 — Feed arrangement for 90° self-phasing of loops.

the quadrifilar, the two bifilar loops require separate excitations having a relative phase difference of 90°. Further, the sense of the 90° phase relationship determines from which end the quadrifilar radiates.

Several different balun and quadrature-phase circuit arrangements are available for feeding the quadrifilar, such as the folded balun, the split-sheath balun, or a combination of 90° and 180° hybrids, and so forth, as described by Bricker and Rickert (*Refs 88, 89*). However, to save weight and to effect simplicity in the construction, a unique feeding arrangement is used. This technique features the infinite, or inherent balun, combined with a novel method of self-phasing the two bifilar loops to achieve the 90° differential current relationship between the loops. The constructional simplicity is apparent in Fig 22-1, which illustrates the quadrifilar configuration used on both the TIROS-N and Air Force 5D satellites, and on the amateur satellite, AMSAT-OSCAR 7.

Sec 22.8 The Infinite or Inherent Balun

In the infinite balun, shown in Fig 22-9, we see the coaxial feed line extending into the loop and shaped to form the first half of a bifilar loop. At the end of the coax, the inner conductor is connected to the opposite or second half of the bifilar loop to form the feed point. The other

end of the second half of the loop is connected to the outside surface of the coax feed line. Thus, the loop is closed at the antipodal point of the loop, where the feed line enters. The second half of the loop is a solid wire of the same diameter as the outer diameter of the coax.

In operation, current flowing on the inner conductor of the coax emerges at the feed point to flow onto the second half of the loop. For current flowing on the inside of the outer conductor of the coax, on its arrival at the end of the coax, the only path for current flow is around the end and onto the outside of the outer conductor. Now such external feed-line current is the desired antenna current, because the outside portion of coax extending from the feed point to the antipodal point is the radiator. Externally, the antipodal point demarks the end of the feed line and the beginning of the loop radiator. Because of skin effect, the transmission line currents flowing inside the coax portion of the loop are completely divorced from the antenna currents flowing externally on the loop. Their only relationship is that the internal transmission-line currents emerge at the feed point, where they become the external antenna currents.

As the feed line is dressed away from the antipodal point symmetrically relative to the loop, currents induced on the feed line because of coupling from each half of the loop are equal and flow in opposite directions. The opposing currents on the

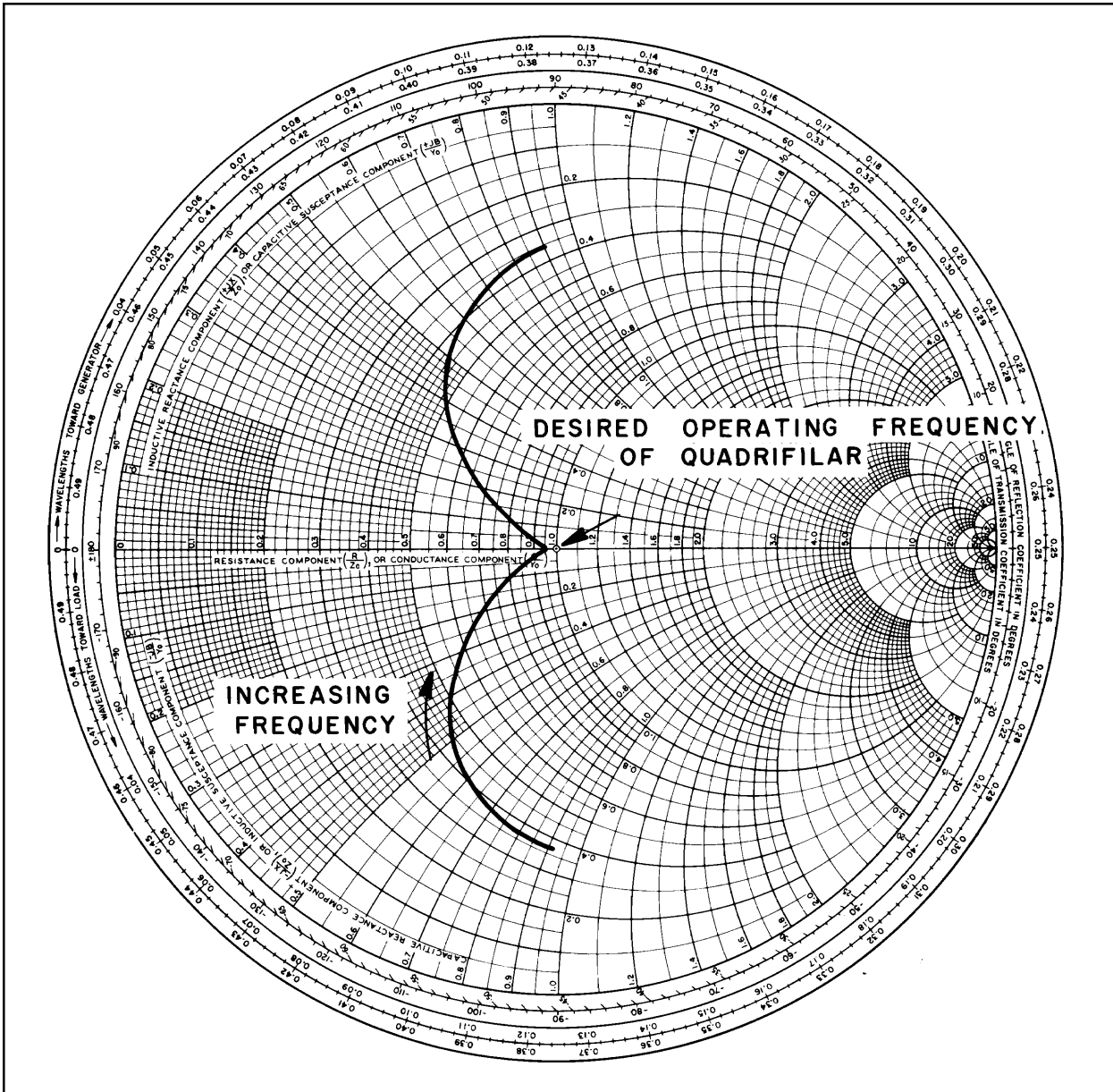


Fig 22-10 — Impedance versus frequency plot of self-phased quadrifilar antenna.

line thus cancel each other, decoupling the feed line from the loop. In other words, from the external viewpoint of the loop radiator, the source generator can be considered to exist directly between the two input terminals of the loop at the feed point, and the feed line effectively disappears. Thus, the current-mode transition in the coaxial-line portion of the loop — from an internal unbalanced mode entering at the antipodal point, to an external balanced mode emerging at the feed point — constitutes an inherent balun device.

Such a device is called an “infinite balun.”

Sec 22.9 Self-Phased Quadrature Feed

As stated, a quadrature-phase current relationship is required between the two bifilar loops of the quadrifilar array. This requirement is met by using the self-phasing method. The orthogonal bifilar loops are designed such that one loop is larger relative to the desired resonant frequency length and therefore inductive, while the other loop is smaller and there-

fore capacitive. Using this method, the two loops are fed in parallel by connecting the terminals of both loops together at the feed point, as shown in Fig 22-9. This self-phasing method requires only one coaxial feed line, and any of the balun arrangements mentioned earlier (shown by Bricker and Rickert, Ref 88) may be used. It is evident that one loop half is the coax feed line, while the other three half loops are simply solid wire.

The larger inductive loop is designed such that, at the operating frequency, the reactive component X_L of the loop terminal impedance is equal to the resistive component, R . Similarly, the smaller capacitive loop is designed so its reactive component X_C equals R at the operating frequency. The $\pm X = R$ relationship is important, because to obtain a relative current phase of 90° between the two loops, the larger loop current must lag by 45° and the smaller must lead by 45° .

For the current phase of the larger loop to lag, or the smaller loop to lead by 45° , their phase angles must be $\pm 45^\circ$, or have an arc tangent of ± 1 . This occurs only when $\pm X = R$. When the two loops are fed in parallel, the relative lag and lead currents in the loops differ in phase by 90° without requiring any additional components to obtain separate differential phase excitations. Dimensions that yield the correct phase relationship with a loop wire diameter of 0.0088λ are as follows.

Smaller loop:

$$D = 0.156 \lambda$$

$$\text{len}_P^\circ = 0.238 \lambda$$

$$\text{Perimeter} = 1.016 \lambda$$

Larger loop:

$$D = 0.173 \lambda$$

$$\text{len}_P^\circ = 0.260 \lambda$$

$$\text{Perimeter} = 1.120 \lambda$$

where

D = diameter of imaginary cylinder on which bifilar is wound len_P° = axial length, as shown in Fig 22-3

The resultant impedance versus frequency response of the parallel-loop combination is shown in the Smith Chart, Fig 22-10. The formation of the cusp in the impedance locus is the design goal that signifies that the 90° phase relationship exists between the loops.

See 22.10 The Quadrifilar in Space

As I've indicated above, the quadrifilar antenna was developed for spacecraft use. Fig 22-11 shows the comparative size between an experimental S-band quadrifilar and the flight-model system of a circularly polarized crossed-dipole antenna over a ground plane, which the quadrifilar replaced. The two antennas have identical radiation characteristics. Four of the crossed-dipole ground-plane units flew on ITOS (TIROS-M). They were replaced with quadrifilars on the newer TIROS-N to save space and weight, but accomplished the same communications tasks on the same frequencies. Using the same technique as described in Sec 22.9 for the quadrifilar, the required 90° dipole phasing to obtain circular polarization in the crossed-dipole array was accomplished by using the short and long dipole elements shown in the picture. The short elements are capacitive, causing the dipole currents to lead by 45° , and the long elements are inductive, causing the currents to lag 45° , resulting in a differential phase of 90° . The balun is a split tube.

Before the launch of OSCAR 7, AMSAT publicized the quadrifilar antenna in the *AMSAT Newsletter* for March 1975 (Ref 131). The cover picture for that issue is included here as Fig 22-12. The

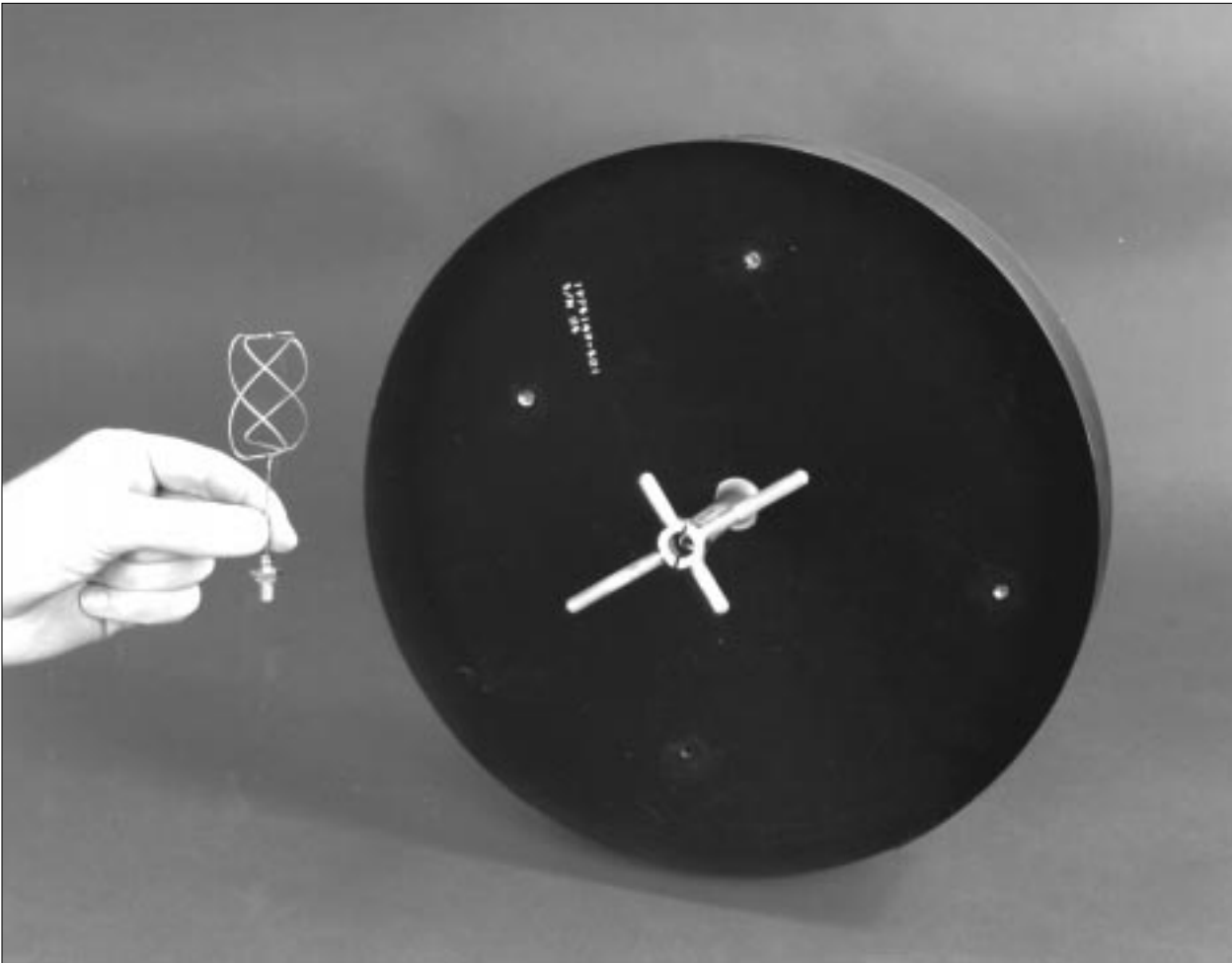


Fig 22-11 — Comparing the size of a quadrifilar antenna and a flight model, circularly polarized crossed dipole over a ground plane system, which it replaced. The two antennas have identical radiation characteristics, but the quadrifilar obviously requires less space and is lighter.

quadrifilar helix antenna is shown mounted on an OSCAR 7 test model at the RCA Space Center, attached to an ITOS weather satellite (TIROS-M) in the piggyback launch configuration. Fig 22-13 shows another view of the test model, while Figs 22-14 and 22-15 show the quadrifilar mounted on the OSCAR 7 spacecraft as it is being readied for flight. In spite of its small size (0.7 ounce), the quadrifilar antenna boasts tremendous performance for spacecraft use. RCA Engineers Randy Bricker, Herb Rickert, and myself developed the original design, for use on the highly successful USAF spacecraft, the Block 5-D Meteorological Satellite, which was built by the RCA

Astro-Electronics Division of Princeton, New Jersey.

The OSCAR 7 antenna is circularly polarized, radiates hemispherically without requiring a ground plane, and has a gain of 5 dBic on axis going down smoothly to 0.0 dBic 90° off axis over the entire 360° around the edge of the hemisphere, with good polarization circularity at the hemisphere edges. It is fed with an infinite balun, and has elements phased at 90° with no phasing line. With a modification I devised to operate at the 2304.1MHz beacon frequency, this antenna was fabricated under the direction of Bricker and myself specifically for the OSCAR 7 amateur spacecraft, and presented to AMSAT

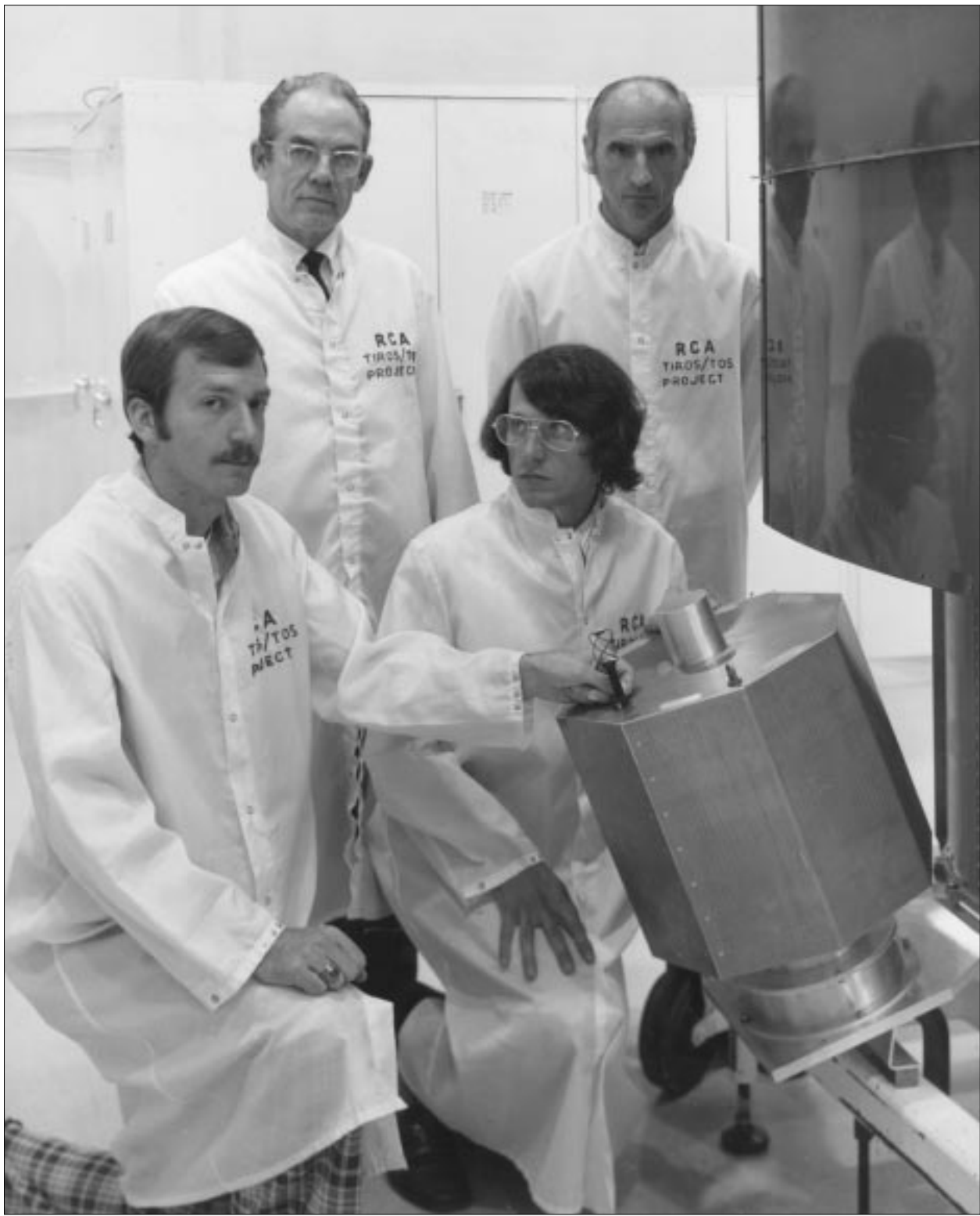


Fig 22-12 — This photo was used as the cover picture for the March 1975 issue of the *AMSAT Newsletter* (Ref 131). Shown clockwise from the upper left are Walt Maxwell (W2DU), Walt Ozman (W2WGH), OSCAR 7 Project Manager and NASA engineer Jan King (W3GEY), and Randy Bricker, who is pointing out the radiation characteristics of the 2304-MHz OSCAR 7 beacon antenna.



Fig 22-13 — The OSCAR 7 quadrifilar on its test model in its piggyback launch configuration alongside the flight-model ITOS spacecraft with which it flew. Left to right are Bricker, Maxwell (W2DU), and Ozman (W2WGH).

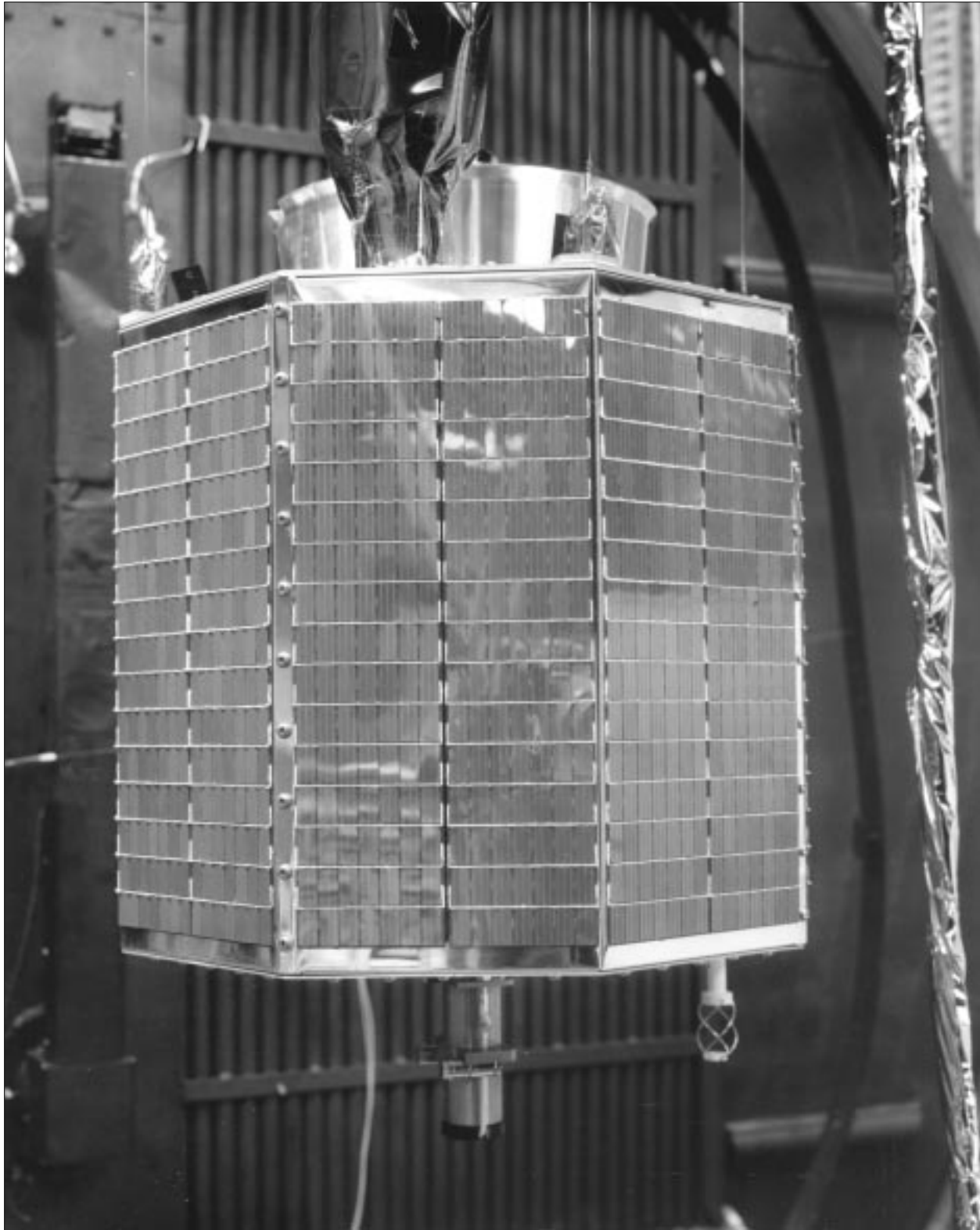


Fig 22-14 — The OSCAR 7 quadrifilar, lower right, mounted on the OSCAR 7 spacecraft during prelaunch readiness operations.

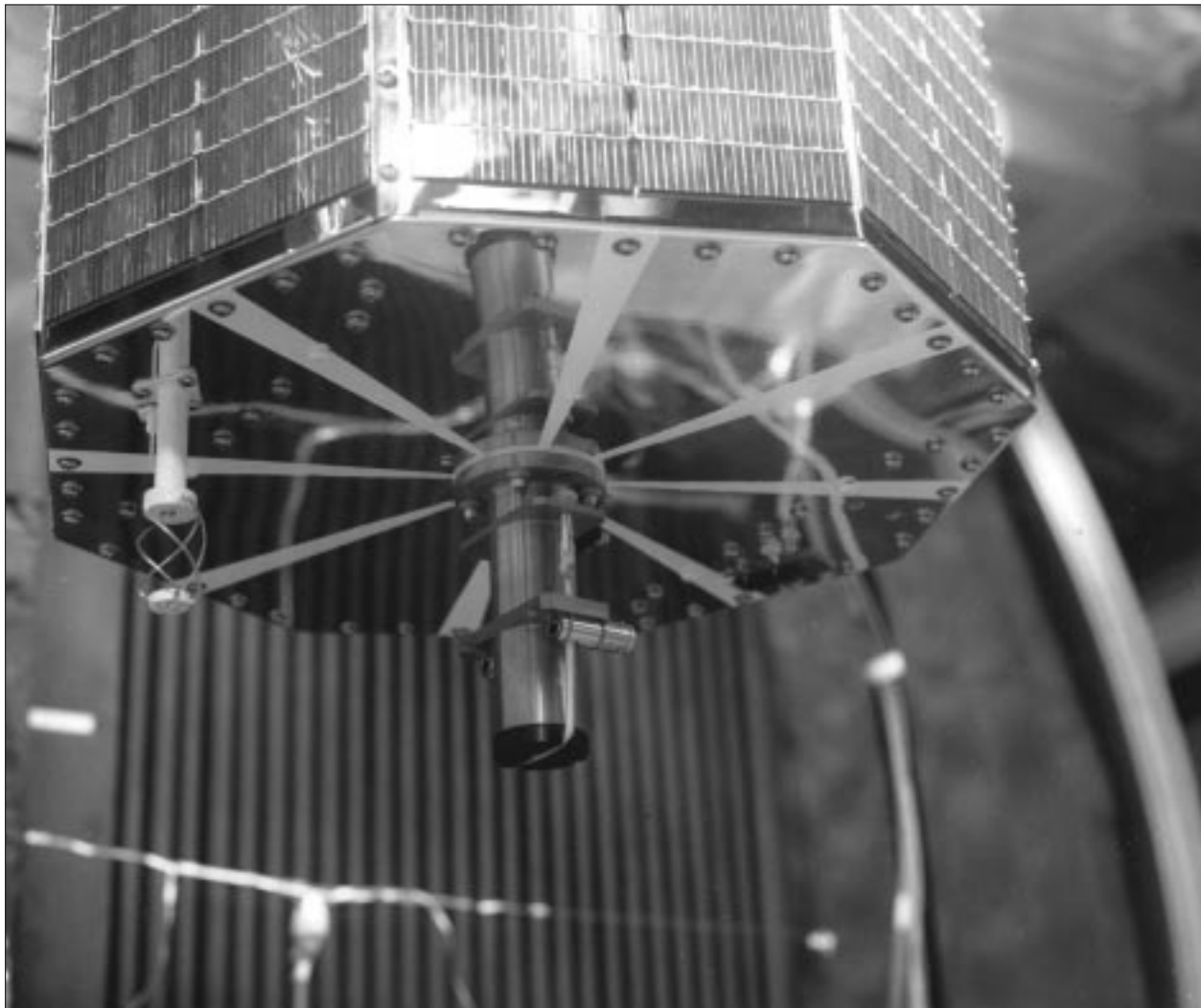


Fig 22-15 — A close-up view of the OSCAR 7 quadrifilar during prelaunch readiness.

by RCA, which designed and built the TIROS-ESSA-ITOS-TIROS-N weather satellite series. (After being accepted by the U.S. Weather Bureau these RCA-built spacecraft became known as NOAA, with a number designation to determine the specific spacecraft of the series.) I also served as consulting engineer for all antenna systems on AMSAT OSCAR 7. RCA Technicians Walt Ozmon, W2WGH, and Joe Rovenski, W2HLO, performed many of the impedance and radiation pattern measurements during the final testing of the OSCAR 7 quadrifilar antenna.

Scaled up for lower frequencies, the quadrifilar has similar performance characteristics. At 146 MHz, the quadrifilar

would form a cylinder approximately 13 inches in diameter and 20 inches high, while at 432 MHz, the diameter and height would be 4.4 inches and 6.8 inches. At 29 MHz the dimensions would be 5.5 feet and 8.4 feet, respectively. The circular polarization reduces polarization fading caused by Faraday rotation of the electric field vector, especially on the 10-meter downlink. The quadrifilar scaled for use at 137 MHz is used quite extensively by weather buffs for receiving APT weather pictures, with excellent results on both 137.5 and 137.62 MHz. One note is of particular importance for those intending to build the quadrifilar. The diameter of the conductors in the bifilar loops is especially

critical. The reason is that the $\pm 45^\circ$ leading and lagging currents in the respective bifilar loops, which obtains the required 90° differential phasing between the two loops, is derived by the corresponding capacitive and inductive reactances in the loops. The distributed inductance in each loop determines the reactance in the loop. When the length of the loop is less than the resonant length the reactance is capacitive, causing the current to lead the voltage. When the loop length is greater than the resonant length the reactance is inductive. Now the critical point: To make the leading current precisely $+45^\circ$ and the lagging current precisely -45° , the distributed inductance of the conductors must also be of precisely the correct value. To obtain the correct value of distributed inductance the length-to-diameter ratio of the conductor also must be correct. The optimum radiation pattern and gain of the antenna requires the leading and lagging currents to be $\pm 45^\circ$. It therefore behooves the builder of the quadrifilar to carefully observe the conductor-diameter requirement to obtain successful operation of the antenna. Using the λ dimension data listed earlier, it may be helpful for the 137 MHz builders to know that 3/4 inch soft copper tubing works very well. Generally, the 137 MHz will allow access of a NOAA weather spacecraft signal at between 5° and 10° in elevation with no nulls during

an entire pass, with continued contact until between 5° and 10° in elevation at the end of the pass. The beauty of the performance of this antenna is that it needs to be no more than $\lambda/4$ above the ground, requires no manipulation or positioning to follow the orbital path of the spacecraft, but it does appreciate a clear shot to the orbital path of the spacecraft. NOAA spacecraft 9 through 13 are presently available for receiving APT pictures in the 137 MHz band.

In summary, the quadrifilar helix antenna differs significantly from the conventional helical antenna. Control of pattern shape and other radiation characteristics are available by selecting appropriate dimensional parameters. A novel balun for feeding this balanced-input device from coaxial feed line is used, as is a method of self-phasing the loop radiating elements to obtain a quadrature current relationship between the loops. The quadrifilar helix is a durable antenna, one that is seeing use on both amateur and commercial satellites, as well as on ground stations for receiving APT weather information transmissions on 137.5 and 137.62 MHz from the TIROS-NOAA weather satellites. The satellites presently transmitting on these APT frequencies are TIROS-N NOAA 9 through NOAA 14.

¹ Among other tasks on the quadrifilar project, I performed the R & D research on more than 1000 different configurations of the quadrifilar helix, which led to the development of the six quadrifilar antennas flying on the polar-orbiting TIROS-N NOAA weather spacecraft. A copy of my research report appears in the Appendix.